

# In vitro biological validation and cytocompatibility evaluation of hydrogel iron-oxide nanoparticles

Cite as: AIP Conference Proceedings **1873**, 020011 (2017); <https://doi.org/10.1063/1.4997140>  
Published Online: 02 August 2017

Enrico Catalano



View Online



Export Citation

## ARTICLES YOU MAY BE INTERESTED IN

[Investigations of the toxic effects of glycans-based silver nanoparticles on different types of human cells](#)

AIP Conference Proceedings **1873**, 020012 (2017); <https://doi.org/10.1063/1.4997141>

[Green synthesis of Ag nanoparticles using plant metabolites](#)

AIP Conference Proceedings **1873**, 020004 (2017); <https://doi.org/10.1063/1.4997133>

[Plasma enhanced hot filament CVD growth of thick carbon nanowall layers](#)

AIP Conference Proceedings **1873**, 020006 (2017); <https://doi.org/10.1063/1.4997135>

**AIP** | Conference Proceedings

Get **30% off** all  
print proceedings!

Enter Promotion Code **PDF30** at checkout



# In vitro Biological Validation and Cytocompatibility Evaluation of Hydrogel Iron-oxide Nanoparticles

Enrico Catalano<sup>1,a)</sup>

<sup>1</sup>Department of Clinical Molecular Biology (EpiGen), Akershus University Hospital, University of Oslo (UiO), Oslo, Norway.

<sup>a)</sup>Corresponding author: [enrico.catalano@medisin.uio.no](mailto:enrico.catalano@medisin.uio.no)

**Abstract.** Superparamagnetic iron oxide nanoparticles (MNPs) have recently been investigated for their excellent biocompatibility as well as multi-purpose biomedical potential with promising results, owing to their ability to be targeted and heated by magnetic fields. In this study, novel hydrogel, chitosan Fe<sub>3</sub>O<sub>4</sub> magnetic nanoparticles were synthesized for possible use for induced magnetic hyperthermia, and targeted drug delivery. The coating of iron oxide nanoparticles plays a key-role to efficiently improve internalization of nanoparticles in many cell types. Targeting is also highly desirable for these applications. In this regard hydrophilic coating like chitosan was used to improve drug release. Uncoated (Fe<sub>3</sub>O<sub>4</sub>) and chitosan-coated iron oxide nanoparticles (CS-Fe<sub>3</sub>O<sub>4</sub>) were synthesized and characterized from the biological point of view. The aim of this study was to provide an *in vitro* evaluation of the cytocompatibility of Fe<sub>3</sub>O<sub>4</sub> and CS-Fe<sub>3</sub>O<sub>4</sub> MNPs by using different *in vitro* evaluation tests. In this context, the cytocompatibility and cytotoxic effects of uncoated and hydrogel chemically-engineered chitosan-coated iron oxide NPs were investigated according to the ISO standard 10993-5:2009. Fe<sub>3</sub>O<sub>4</sub> and CS-Fe<sub>3</sub>O<sub>4</sub> NPs were tested on human mammary epithelial cells (MCF-10A) by using direct and not direct contact cytotoxicity evaluation tests, by evaluating influence of the iron particles on the cytoskeleton with phalloidin/DAPI staining and *in vitro* cellular iron uptake with Perl's Prussian blue staining. The results indicate that uncoated and chitosan-coated iron oxide nanoparticles are cytocompatible, without negative influence on the cytoskeleton or higher accumulation of iron in the cytoplasm. Therefore, it is encouraging that our data suggest uncoated and chitosan-coated iron oxide nanoparticles have satisfactory proliferative and viability effects on MCF-10A cells. In conclusion data suggest that both MNP types may be differently aimed in biomedical application in relation to the dose, acting as biocompatible materials, as component of scaffolds, or as a device for theranostics.

## INTRODUCTION

Nanomaterial structures with dimensions between 1 and 100 nm are currently used for medical applications; such as magnetic drug targeting, hyperthermia, and enhanced resolution magnetic resonance imaging [1]. Nanomedicine formulations aim at improving distribution and accumulation at the target sites [2]. Hence, nanomaterials could improve the therapeutic index of low molecular weight drugs and provide more effective and less toxic treatment [3]. However, levels of inorganic nanoparticles (NPs) have already increased in ambient air and have impacted public health [1, 2, 4]. Previous studies revealed that NP, such as iron oxide NPs, can enter into cells and accumulate in mitochondria, vesicles, phagosomes and lysosomes [5, 6].

The use of magnetic nanoparticles (MNPs) is gaining ground in various industrial domains [7]. Iron oxide nanoparticles are the most commonly used magnetic nanoparticles and their use shows promise in a number of biomedical applications. The use of MNPs for delivery of drugs is also promising. When an external magnetic field and field gradient are applied, active ingredients bound to or incorporated in these particles are successfully carried to the desired site with relatively high accuracy, minimum surgical intervention, maximum dose, and avoidance of toxic side effects on other organs [8]. Because of the possibility of inducing magnetization by applying an external magnetic field, thus directing them to a target site, and heating them by applying an external alternating current

magnetic field, they are particularly promising for many biomedical applications and cancer therapy [9]. The precise control of the physiochemical and biological properties of these magnetic systems is crucial for their biomedical applications, as the induced heat is highly dependent on these properties and useful for targeting magnetic drug release. Due to their unique magnetic properties, excellent biocompatibility as well as multi-purpose biomedical potential superparamagnetic iron oxide nanoparticles (SPIONs) are attracting increasing attention in both pharmaceutical and industrial communities. These include both *in vitro* technologies (diagnostic separation, selection, and magnetorelaxometry) [10], and *in vivo* innovative therapeutic (hyperthermia and drug-targeting) and diagnostic approaches (nuclear magnetic resonance – NMR- imaging) [11]. Iron oxide nanoparticles can be engineered with desired functionality. The techniques used for surface functionalization comprise grafting of or coating with organic species, including surfactants or polymers [12]. The coating of MNPs plays a key-role to efficiently improve internalization of NPs in many cell types. Targeting is also highly desirable for these applications. Strong magnetization and the ability to functionalize surfaces with targeting moieties are the keys to improve MNPs effectiveness. In this perspective we used a hydrophilic coating like chitosan to favor drug release in the target site. Chitosan is a deacetylated derivative of chitin, a positively charged natural polymer carrier found in the shells of crustaceans, and is structurally similar to hyaluronic acid (extracellular matrix) [13, 14]. The biomedical applications of chitosan have been studied for over 40 years [13]. The excellent properties of chitosan, including its biocompatibility, bioactivity, biodegradability, and nontoxic byproducts make it easy to functionalize for biomedical applications [13]. The cell adhesion and potential uptake of chitosan particles are also most favorable due to their attraction to negatively charged cell membranes, an attractive feature for the treatment of solid tumors [15]. Moreover, chitosan has shown favorable biocompatibility [16] as well as the ability to increase cell membrane permeability both *in vitro* and *in vivo* [17]. Among the various biopolymers, chitosan along with nanoparticles has been utilized as a stabilizing agent due to its excellent film-forming ability, mechanical strength, biocompatibility, non-toxicity, high permeability towards water, susceptibility to chemical modifications, cost-effectiveness [18]. So the chitosan layer in the magnetic nanoparticles is useful for the functionalization and the biocompatibility of this type of nanoparticles, in particular by avoiding the possible release of toxic substances from the core of magnetite ( $\text{Fe}_3\text{O}_4$ ) crystalline structure.

In this context, we examined the cytotoxic effects of uncoated and hydrogel chemically-engineered chitosan-coated iron oxide NPs by using different *in vitro* direct and not direct evaluation tests of cell biocompatibility by evaluating influence of the iron particles on the cytoskeleton with phalloidin/DAPI staining and *in vitro* cellular iron uptake with Perl's Prussian blue staining.

## MATERIALS AND METHODS

### Synthesis of Iron Oxide Nanoparticles

Magnetic iron oxide nanoparticles ( $\text{Fe}_3\text{O}_4$ ) were prepared by alkaline co-precipitation of ferrous chloride tetrahydrate,  $\text{FeCl}_2 \cdot 4\text{H}_2\text{O}$  (1.34 g) (Sigma-Aldrich) and ferric chloride hexahydrate  $\text{FeCl}_3 \cdot 6\text{H}_2\text{O}$  (3.40 g) (Sigma-Aldrich) at 1:2 ratio. The salts were dissolved in 150 mL deionized water within a three necked glass balloon. The glass balloon was placed in a heating mantle and stirred with a magnetic stirrer. It was vigorously stirred at 90°C in the presence of  $\text{N}_2$  gas. Ammonium hydroxide ( $\text{NH}_4\text{OH}$ ) (Sigma-Aldrich) was added to the system drop wise. The process was ended by washing with deionized water until the solution pH was 9.0. The solution was then centrifuged at 5000 rpm for 30 minutes. The precipitates were collected and dried in the incubator (Thermo Fisher Scientific, Waltham, Massachusetts, U.S.) at 55°C. The black precipitates were then turned into brown.

### Synthesis of Chitosan-coated Magnetic Iron Oxide Nanoparticles

Chitosan-coated magnetic iron oxide nanoparticles ( $\text{CS-Fe}_3\text{O}_4$ ) were in situ synthesized by the co-precipitation of Fe (II) and Fe (III) salts in the presence of chitosan (Sigma-Aldrich) and trisodium phosphate molecules (Sigma-Aldrich). Chitosan was previously prepared with degree of deacetylation 75% by titrimetric method [19]. Trisodium phosphate was used for the crosslinking of low molecular weight chitosan polymers. Chitosan (0.15 g) was dissolved in 30 ml of 1% acetic acid (Sigma-Aldrich) and the pH was adjusted to 4.8 by 10M NaOH (Sigma-Aldrich). Iron salts (1.34 g  $\text{FeCl}_2 \cdot 4\text{H}_2\text{O}$  and 3.40 g  $\text{FeCl}_3 \cdot 6\text{H}_2\text{O}$ ) were dissolved in 30 ml of 0.5% chitosan solution. The solution was then vigorously stirred at 2000 rpm. 10 ml of 22.5% trisodium phosphate and different amounts of 32%  $\text{NH}_4\text{OH}$  (18, 20, 22, 25 mL) (Sigma-Aldrich) were added to the solution to obtain the final  $\text{NH}_4\text{OH}$  concentration of 31%, at room temperature. The ammonia solution was added very slowly to produce smaller sized

nanoparticles. The resulting solution was stirred for an additional 1 hour. The colloidal chitosan coated magnetic Fe<sub>3</sub>O<sub>4</sub> nanoparticles were extensively washed (3 times) with deionized water and separated by centrifugation and drying.

### Cell cultures

Human mammary epithelial cells (MCF 10A, ATCC, CRL-10317) was cultivated in Mammary Epithelial Cell Growth Medium (MEGM, Lonza/Clonetics) supplemented with 2 mM L-glutamine(Lonza/Clonetics), 100 ng/ml cholera toxin (Sigma-Aldrich), 10% fetal bovine serum (FBS, Gibco, Thermo-Fisher, Pittsburg, PA, US) and 1% antibiotics/antimycotics (penicillin/streptomycin/gentamycin, Gibco) (complete medium). Cells were incubated in a humidified 5% CO<sub>2</sub> atmosphere at 37°C and passaged twice weekly at a 1:4-5 concentration.

### Lactate dehydrogenase assay

The effect of the NPs on the integrity of the cell membrane was assayed using a LDH Cytotoxicity Assay Kit (Gesan group, Italy). The assay was performed as per the manufacturer's instructions. LDH is released by cells in response to damage or loss of integrity of cell membrane and is a cellular toxicity indicator. Briefly, 1.6 ×10<sup>4</sup> MCF-10A cells/well were seeded in 24-well plates and treated with the following concentrations of MNPs: 10 µg/ml, 20 µg/ml, 40 µg/ml and 80 µg/ml (w/v) for 24, 48 and 72 hours. Untreated cells were taken as the negative control and cells treated with lysis buffer were taken as the high control (total LDH in the cell). As a positive control, 1 µL of LDH was used to validate the assay. Following the incubation with NPs, the well plates were centrifuged at 600 g for 10 minutes and 10 µL of the medium was transferred to a fresh 96-well plate. The medium was then incubated with 100 µL of LDH reaction mixture for 15 minutes at room temperature and the absorbance was measured at 450 nm using the microplate reader (Victor X4 - PerkinElmer) with the reference wavelength at 650 nm. LDH was quantified using the following formula:

$$\text{LDH\%} = \frac{\text{Test-Low control}}{\text{High control-Low control}} \times 100 \quad (1)$$

in which “low control” was the cells without any treatment and “high control” was the cells treated with lysis buffer (total LDH).

### Direct contact cytotoxicity evaluation

Direct static contact cytotoxicity of MNPs was evaluated following the ISO standard 10993-5:2009 on Biological Evaluation of Medical Devices instructions [3]. Cells were seeded in 24-well plates (1.6 × 10<sup>4</sup> cells per well) in complete MEGM medium and incubated for 24 h at 37°C in 5% CO<sub>2</sub>. Medium containing MNPs at 10, 20, 40 and 80 µg/ml (w/v) was added to cultures, replacing the old medium. Fresh medium without MNPs was used as control. Cell viability was evaluated after 24, 48 and 72 hours by the (3-(4,5-Dimethylthiazol-2-yl)-2,5-diphenyltetrazolium bromide colorimetric assay (MTT, Sigma). Briefly, 100 µl of MTT solution (3 mg/ml in PBS) were added to each specimen and incubated for 4 hours in the dark at 37°C; formazan crystals were then dissolved in 100 µl of dimethyl sulphonylde (DMSO, Sigma- Aldrich) and 50 µl were collected and centrifuged to remove any debris. Supernatant optical density (o.d.) was evaluated at 570 nm (Spectrophotometer, Packard Bell, Meriden, CT, USA). The mean optical densities obtained from control specimens were taken as 100% viability. Cell viability was calculated as follow: (experimental o.d. / mean control o.d.)\*100. Experiments were performed with four replicates at each experimental time.

### Leaching toxicity tests of MNPs

For leaching toxicity tests the MNPs were sterilized with UV and MEGM culture medium containing 10% calf serum was then added to it in a sterile closed vessel (final concentration 0.1 g/mL). Leaching conditions were 37°C over 72 hours. The samples were then centrifuged at 2500 rpm for 5 minutes, the supernatant was removed by suction and filtered through a microporous filter (VWR International, U.S.) to provide a 100% leach solution.

During the test, the MEGM culture medium was diluted to the required concentration. MCF-10A cells were removed during their logarithmic growth phase and digested in the cell suspension; the cell concentration was next adjusted to  $4 \times 10^3/\text{mL}$  and inoculated on a 96-well culture plate at 200  $\mu\text{L}/\text{well}$ . The sample was cultured in an incubator at 37°C under saturated humidity and 5% CO<sub>2</sub> conditions. The primary solution was discarded after 24 hours, at which time the leaching solution was added until the final concentration was 100%, 75%, 50%, and 25%. The MEGM culture inoculum was used as control. Each group comprising four wells was cultured for 72 hours, and 20  $\mu\text{L}$  of MTT was then added into each well and incubated for 4 hours. The absorbance value was measured at 570 nm using a spectrophotometer (Packard Bell, Meriden, CT, USA). The relative cell growth rate was calculated as follows: relative growth rate % = OD (Optical Density) mean value of test group/OD mean value of negative control group  $\times 100\%$ .

### Cell morphology evaluation

Cells were seeded on glass coverslips (12 mm diameter) in 24-well plates, and after 24 h they were incubated with MNPs for 72 h at the concentrations described above. Cells were then fixed with 4% paraformaldehyde (Sigma-Aldrich) in phosphate buffered saline (PBS) for 20 minutes at 4 °C, washed 3 times with PBS, and permeabilized with 0.2% Triton X-100 (Sigma-Aldrich), 1% bovine serum albumin (BSA), and 5% goat serum in PBS for 2 h. Tetramethyl Rhodamine B isothiocyanate (TRITC)-Phalloidin (1/2000 in PBS, AbCam, Cambridge, UK) was added for 45 minutes at room temperature; specimens were then washed thrice more with PBS and nuclei were stained with 4',6-diamidino-2-phenylindole (DAPI, Sigma-Aldrich). Immunofluorescence(IF) images were acquired with fluorescent microscope (Leica AF 6500, Leica Microsystems, Basel, CH) at 20x magnification.

### *In vitro* cellular iron uptake studies – Perl's Prussian blue staining

MCF-10A cells at a density of  $5 \times 10^5$  cells/well were seeded onto the 12-well plate and incubated for 24 h, and 1 mL of the DMEM containing Fe<sub>3</sub>O<sub>4</sub> or CS-Fe<sub>3</sub>O<sub>4</sub> NPs (Fe concentration was fixed to be 40  $\mu\text{g}/\text{mL}$ ) were added and incubated at 37°C for 24 h. After incubation the cells were fixed with 4% paraformaldehyde(PF). Then Perl's Prussian blue staining assay was performed according to the following method. The PB solution was prepared by mixing 3 mL of 2% potassium ferrocyanide (II)(Merck) with the same amount of 1% hydrochloric acid (Merck). The stain was then put on the cells at room temperature for 20 min. Nuclear fast redaluminumsulphate staining(Sigma-Aldrich) was performed to colour the nuclei. The wells without Fe<sub>3</sub>O<sub>4</sub> or CS-Fe<sub>3</sub>O<sub>4</sub> NPs were used as control. Perl's Prussian blue staining images were taken on an Olympus BX51 optical microscope at 100x magnification(Olympus Corp, Tokyo, Japan). Perl's Prussian blue was performed to control the intracellular accumulation of iron ions in mammary epithelial cells after contact with magnetic nanoparticles

### Statistical analyses

All statistical analyses were performed using the IBM Statistical Package for Social Sciences v. 20 (SPSS – IBM, Chicago, MI, US). Multiple comparisons were analyzed using Levene's test, one way analysis of variance (ANOVA) followed by Scheffe's test. Two-samples comparisons were evaluated with the Mann-Whitney U test. P values < 0.05 were considered to be statistically significant.

## RESULTS

### Lactate dehydrogenase assay

The lactate dehydrogenase assay is able to evaluate cell damage, as indicated by lactate dehydrogenase release from the cytosol of lysed cells. LDH leakage from MNPs reflects cell membrane disruption. The lactate dehydrogenase results on MCF-10A cells were consistent with those of direct contact cytotoxicity (Fig. 1). All types of MNPs stimulated LDH release in a concentration-dependent manner. LDH release of Fe<sub>3</sub>O<sub>4</sub> NPs and CS-Fe<sub>3</sub>O<sub>4</sub> NPs (in a range between 3.09 and 5.13%) was limited compared to control after 24, 48 and 72 hours, suggesting less cell membrane damage (Fig. 1). Data were considered statistically significant ( $p < 0.05$ ).

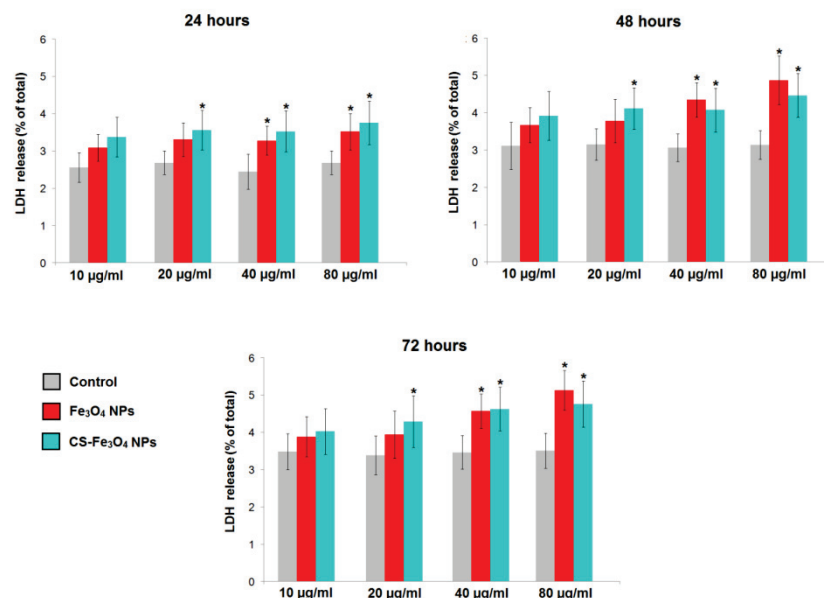


**Figure 1.** Effect of MNPs on cell-membrane integrity following exposure to increasing concentrations of MNPs for 24, 48 and 72 hours. The relative lactate dehydrogenase (LDH) release was co-related to percentage cytotoxicity. Data are shown as the mean  $\pm$  standard deviation (n = 4). \*P < 0.05 compared with control.

#### Material toxicity testing of magnetic nanoparticles leach solution

The values of cell viability revealed no significant difference in MCF-10A cell growth compared with that in the control group after Fe<sub>3</sub>O<sub>4</sub> and CS-Fe<sub>3</sub>O<sub>4</sub> nanoparticle leaching solution (100%, 75%, 50%, and 25%) was added. The relative growth rate is shown in Table 1. The results indicate that the 100% leaching solution of Fe<sub>3</sub>O<sub>4</sub> nanoparticles is cytocompatible toward MCF-10A cells. Considering the relative growth rate, the eluates solutions of Fe<sub>3</sub>O<sub>4</sub> and CS-Fe<sub>3</sub>O<sub>4</sub> nanoparticles showed a cell viability on MCF-10A cells comparable to control.

Fe <sub>3</sub> O <sub>4</sub> nanoparticles			CS-Fe <sub>3</sub> O <sub>4</sub> nanoparticles		
Groups	OD	Relative growth rate (%)	Groups	OD	Relative growth rate (%)
Control	0.289 $\pm$ 0.005	100	Control	0.289 $\pm$ 0.005	100
25% extract liquid	0.277 $\pm$ 0.004	95.9	25% extract liquid	0.280 $\pm$ 0.008	97.1
50% extract liquid	0.271 $\pm$ 0.006	93.8	50% extract liquid	0.273 $\pm$ 0.005	94.6
75% extract liquid	0.261 $\pm$ 0.008	90.6	75% extract liquid	0.266 $\pm$ 0.007	92.1
100% extract liquid	0.254 $\pm$ 0.006	87.8	100% extract liquid	0.257 $\pm$ 0.006	88.9

**Table 1.** Leaching extract solutions for Fe<sub>3</sub>O<sub>4</sub> and CS-Fe<sub>3</sub>O<sub>4</sub> nanoparticles.

## Direct contact cytotoxicity

For MCF-10A cells the cell viability after 24 hours (MTT assay) range between 80% and 96% for Fe<sub>3</sub>O<sub>4</sub>, 88% and 92% for CS-Fe<sub>3</sub>O<sub>4</sub> (Fig.2). The cell viability after 48 hours (MTT assay) range between 83% and 95% for Fe<sub>3</sub>O<sub>4</sub>, 90% and 94% for CS-Fe<sub>3</sub>O<sub>4</sub> (Fig.2). The cell viability after 72 hours (MTT assay) range between 82% and 94% for Fe<sub>3</sub>O<sub>4</sub>, 89% and 91% for CS-Fe<sub>3</sub>O<sub>4</sub> (Fig.2). Fe<sub>3</sub>O<sub>4</sub> and CS-Fe<sub>3</sub>O<sub>4</sub> MNPs did not affect the viability of mammary epithelial cells in a range of concentration of MNPs from 10 to 80 µg/ml. Cell viability slightly decreased at higher concentrations, and for longer contact times. In all cases, viability was above 80%. These data of cell viability showed cytocompatibility and stability of the chitosan layer of nanoparticles comparable to control.

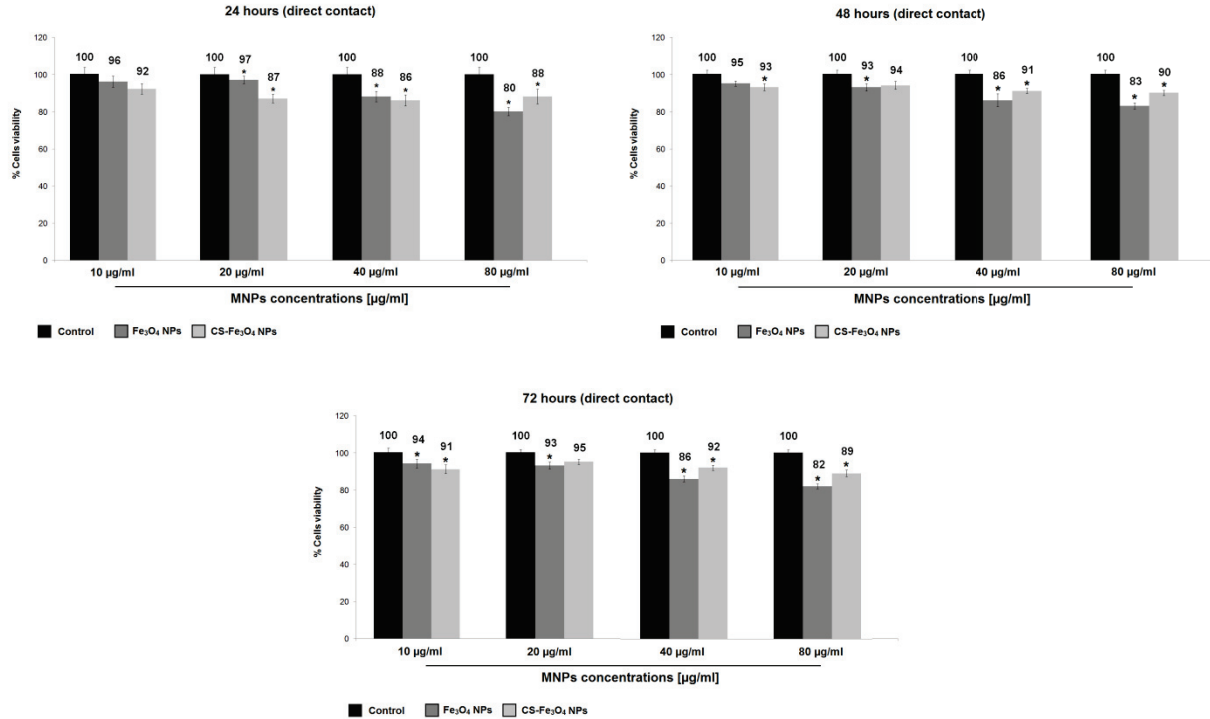


**Figure 2.** Direct contact cytotoxicity evaluation of MNPs using mammary epithelial cells (MCF-10A cells) at different time points. Data are shown as the mean  $\pm$  standard error of the mean (n = 4). \*P < 0.05 compared with control samples.

## Cell morphology evaluation

Compared to untreated controls, no morphological alterations of the cells were observed after direct contact with MNPs for 72 h (Fig. 3A). IF staining allowed to observe a regular cell morphology of mammary epithelial cells in contact with magnetic nanoparticles respect to control (Fig.3A). This indicates that iron-oxide nanoparticles haven't an adverse effect on cell morphology and consequently on the cytoskeleton. As a further confirmation, cells fluorescence intensity (data not shown) was comparable between untreated controls and MNPs loaded cells and no statistically significant differences were noticed at each time-points (p>0.05).

## *In vitro* cellular iron uptake studies

Internalization of the Fe<sub>3</sub>O<sub>4</sub> and CS-Fe<sub>3</sub>O<sub>4</sub>NPs was confirmed by Prussian blue staining, a method that gives a characteristic blue color in the presence of ferric ions. The results of the staining studies indicate that the intracellular presence of Fe<sub>3</sub>O<sub>4</sub> can be visualized by the positive blue spots in MCF-10A cells compared to control (Fig. 3B). Reduced accumulation of intracellular iron was observed for both types of nanoparticles: Fe<sub>3</sub>O<sub>4</sub> and CS-Fe<sub>3</sub>O<sub>4</sub> compared to control (Fig. 3B).

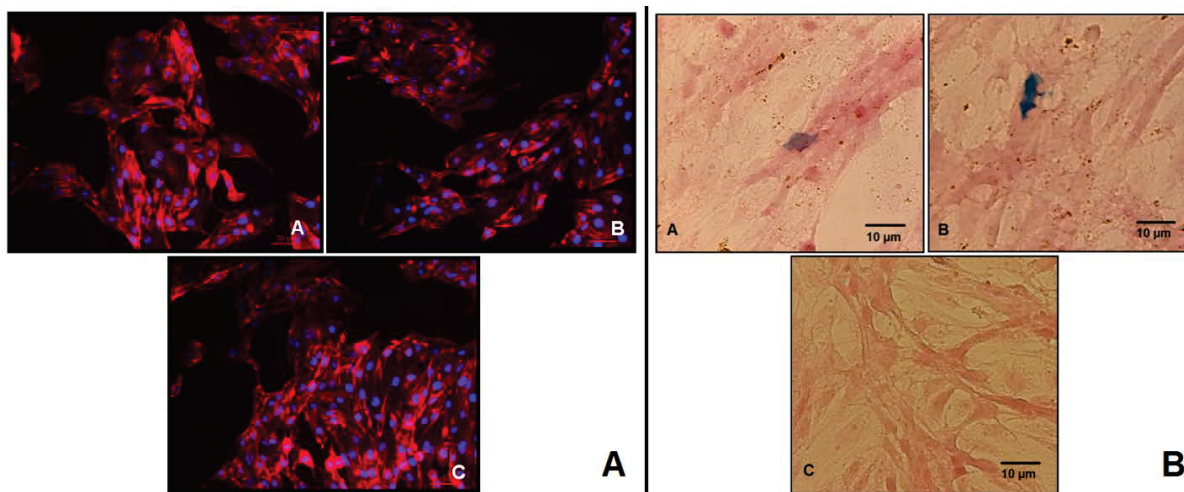


**Figure 3A.** MCF-10A cells in contact for 72 h with Fe<sub>3</sub>O<sub>4</sub> (a), CS-Fe<sub>3</sub>O<sub>4</sub> NPs (b), and Control (c). (40 μg/ml). IF staining with DAPI (blue) and phalloidin (red). Magnification: 20x, bar scale = 50 μm; **3B.** Prussian Blue staining of MCF-10A cells seeded for 72 h in contact with Fe<sub>3</sub>O<sub>4</sub> (a), CS-Fe<sub>3</sub>O<sub>4</sub> NPs (b), and Control (c). Magnification: 100x, bar scale = 10 μm.

## DISCUSSION AND CONCLUSION

As nanotechnology has developed, several methods, both physical and chemical, have been proposed to prepare MNPs [7]. There are advantages and disadvantages to each method; moreover, information concerning the toxicity of MNPs is still incomplete, and different studies apply different test protocols, making their comparison difficult [7]. The ability of magnetic nanoparticles to be functionalized and concurrently respond to a magnetic field has made them a useful tool for theranostics – the fusion of therapeutic and diagnostic technologies that targets to individualize medicine [20].

Fe<sub>3</sub>O<sub>4</sub> are superior to other metal oxide nanoparticles for their non-toxicity, biocompatibility, magnetic properties and chemical stability and are, by far, the most commonly employed MNPs for biomedical applications. Recently, considerable research has been focused on iron oxides due to their potential uses such as magnetic drug targeting, magnetic resonance imaging for clinical diagnosis, recording material and catalysts [21]. Surface modification can stabilize magnetite nanoparticles in the physiological environment and functionalize them to make them responsive to the physical stimuli [22]. The relevance of the prepared chitosan-coated MNPs as a successful candidate for multifunctional nanoprobes is important for the delivery of the magnetic materials inside cellular environment. The aim of this study was to provide an *in vitro* evaluation of the cytocompatibility of Fe<sub>3</sub>O<sub>4</sub> and CS-Fe<sub>3</sub>O<sub>4</sub> MNPs. Uncoated and chitosan-coated iron oxide nanoparticles were synthesized and characterized from the biological point of view. The results indicate that chitosan-coated iron oxide nanoparticles are cytocompatible. Chemotherapy drugs could be also loaded into chitosan-coated nanoparticles; the magnetic properties of these nanoparticles can be utilized to target the infective focus, resulting in a high drug concentration at the appropriate site. Thus, the success of such a treatment requires that the particles are cytocompatible with cells. Therefore, it is encouraging that our data suggest uncoated and chitosan-coated iron oxide nanoparticles in conditions of direct contact have satisfactory proliferative and viability effects on MCF-10A cells. Fe<sub>3</sub>O<sub>4</sub> and CS-Fe<sub>3</sub>O<sub>4</sub> NPs were also demonstrated to be cytocompatible in not direct contact cell model by using eluates solution of cell culture media in contact with MNPs to control the release of possible toxic substances. Moreover, phalloidin/DAPI staining showed no negative influence of the iron particles on the cytoskeleton. This is of great importance considering the essential role of the cytoskeleton in migration capability and cell division. The biocompatible surface coating not only stabilizes the iron oxide nanoparticles, but also provides accessible surface for the biomolecular conjugation through the well-developed bioconjugation chemistry for biomedical applications [23]. In addition, multiple grafting or coating of small molecules can provide multivalent systems that exhibit significantly enhanced efficacy towards the drugs and biomolecules [24]. Hydrogel chitosan-coated MNPs with higher properties of hydrophilicity are the most optimal choice for use as anticancer agents due to their unusual beneficial properties, most notably enhanced drug

availability for prolonging the drug effects in tumor tissues [24]. These results are promising for applications in biomedicine, but further *in vivo* and *in vitro* investigations of the efficacy and safety of these hydrogel magnetic nanoparticles are necessary to optimize their use in various applications like targeted drug delivery for anticancer therapy.

## ACKNOWLEDGMENTS

The research leading to these results has received funding from the European Union Seventh Framework Programme (FP7-PEOPLE-2013-COFUND) under grant agreement n° 609020 - Scientia Fellows.

## REFERENCES

1. A. D. Maynard, R. J. Aitken, T. Butz, et al. Safe handling of nanotechnology. *Nature*. (2006);444:267-269.
2. S. Lanone, J. Boczkowski. Biomedical applications and potential health risks of nanomaterials: molecular mechanisms. *CurrMol Med*. (2006); 6:651-663.
3. J. B. Hall, M. A. Dobrovolskaia, A. K. Patri, S. E. McNeil. Characterization of nanoparticles for therapeutics. *Nanomedicine (Lond)*. (2007); 2:789-803.
4. V. L. Colvin. The potential environmental impact of engineered nanomaterials. *Nat Biotechnol*. (2003); 21:1166-1170.
5. T. Xia, M. Kovoichich, J. Brant, et al. Comparison of the abilities of ambient and manufactured nanoparticles to induce cellular toxicity according to an oxidative stress paradigm. *Nano Lett*. (2006); 6:1794-1807.
6. A. Gojova, B. Guo, R. S. Kota, J. C. Rutledge, I. M. Kennedy, A. I. Barakat. Induction of inflammation in vascular endothelial cells by metal oxide nanoparticles: effect of particle composition. *Environ Health Perspect*. (2007); 115:403-409.
7. D. L. Huber. Synthesis, properties, and applications of iron nanoparticles. *Small* (2005); 1:482-501.
8. B. Polyak, G. Friedman. Magnetic targeting for site-specific drug delivery: applications and clinical potential. *Expert Opin Drug Deliv*. (2009); 6(1):53-70.
9. M. Hofmann-Antenbrink, B. von Rechenberg, H. Hofmann. Superparamagnetic nanoparticles for biomedical applications. In: *Nanostructured Materials for Biomedical Applications*. Transworld Research Network, India, (2009); 119-149.
10. S. Schwarz, J.E. Wong, J. Bornemann, M. Hodenius, U. Himmelreich, et al. Polyelectrolyte coating of iron oxide nanoparticles for MRI-based cell tracking. *NanomedNanotechnol*. (2012); 8:682-691.
11. Z. Li, M. Kawashita, N. Araki, M. Mitsumori, M. Hiraoka, M. Doi. Magnetite nanoparticles with high heating efficiencies for application in the hyperthermia of cancer. *Mater SciEng C* (2010); 30:990-996.
12. S. Chandra, S. Mehta, S. Nigam, D. Bahadur. Dendritic magnetite nanocarriers for drug delivery applications. *New J Chem*(2010); 34:648-655.
13. G. L. Jones, A. Motta, M. J. Marshall, A. J. El Haj, S. H. Cartmell. Osteoblast: osteoclast co-cultures on silk fibroin, chitosan and PLLA films. *Biomaterials*. (2009); 30(29):5376-5384.
14. S. Mathews, P. K. Gupta, R. Bhonde, S. Totey. Chitosan enhances mineralization during osteoblast differentiation of human bone marrow-derived mesenchymal stem cells, by upregulating the associated genes. *Cell Prolif*. (2011); 44(6):537-549.
15. Y. Xu, Y. Du. Effect of molecular structure of chitosan on protein delivery properties of chitosan nanoparticles. *Int J Pharm* (2003); 250:215-226.
16. P. Artursson, T. Lindmark, S.S. Davis, L. Illum. Effect of chitosan on the permeability of monolayers of intestinal epithelial cells (Caco-2). *Pharm Res* (2004); 11:1358-1361.
17. R. Fernández-Urrusuno, P. Calvo, C. Remuñán-López, J. L. Vila-Jato, M. J. Alonso. Enhancement of nasal absorption of insulin using chitosan nanoparticles. *Pharm Res* (1999); 16:1576-1581.
18. Y. Miao, S. N. Tan. Amperometric hydrogen peroxide biosensor based on immobilization of peroxidase in chitosan matrix crosslinked with glutaraldehyde. *Analyst* (2000); 125:1591-1594.
19. L.F. Qi, Z.R. Xu, X. Jiang. Preparation and antibacterial activity of chitosan nanoparticles. *Carbohydr Res* (2004); 339:2693-2700.
20. E.H. Kim, H.S. Lee, B.K. Kwak, B.K. Kim. Synthesis of ferrofluid with magnetic nanoparticles by sonochemical method for MRI contrast agent. *J MagnMagn Mater* (2005); 289:328-330.
21. S.W. Hong, Y. Chang, M.J. Hwang, I. Rhee, D.S. Kang. Ni-Fe<sub>2</sub>O<sub>4</sub> nanoparticles as contrast agents for magnetic resonance imaging. *J Korean SocMagnReson Med* 2004; 4:27-32.
22. J. Ren, M. Jia, T. Ren, W. Yuan, Q. Tan. Preparation and characterization of PNIPAAm-b-PLA/Fe<sub>3</sub>O<sub>4</sub> thermo-responsive and magnetic composite micelles. *Mater Lett* (2008); 62:4425-4427.
23. Y. Sahoo, H. Pizem, T. Fried, D. Golodnitsky, L. Burstein, S.N. Sukenik, G. Markovich. Alkyl phosphonate/phosphate coating on magnetite nanoparticles: a comparison with fatty acids. *Langmuir* (2001); 17:7907-7911.
24. C. Fonseca, S. Simões, R. Gaspar. Paclitaxel-loaded PLGA nanoparticles: preparation, physicochemical characterization and *in vitro* anti-tumoral activity. *J Control Release* (2002); 83:273-286.